Chapter

New Bismuth Sodium Titanate Based Ceramics and Their Applications

Hengchang Nie, Genshui Wang and Xianlin Dong

Abstract

Ferroelectric materials are widely investigated due to their excellent properties and versatile applications. At present, the dominant materials are lead-containing materials, such as Pb (Zr,Ti)O_3 solid solutions. However, the use of lead gives rise to environmental concerns, which is the driving force for the development of alternative lead-free ferroelectric materials. $(Bi_{0.5}Na_{0.5})TiO_3$-based ceramics are considered to be one of the most promising lead-free materials to replace lead-containing ferroelectric ceramics due to their excellent ferroelectric properties, relaxation characteristics, and high Curie point. After decades of efforts, great progress has been made in the phase structure characterization and properties improvement of BNT based ceramics. However, most of the studies on BNT system mainly focuses on its piezoelectric properties and application of piezoelectric sensors and strain actuators, little attention is paid to its ferroelectric properties and related applications. In this chapter, new BNT-based ceramics via composition modification and special focuses on the ferroelectric properties, phase transition behaviors under external fields and related applications, such as application in energy storage, pulsed power supply and pyroelectric detection were proposed.

Keywords: bismuth sodium titanate, ferroelectric properties, energy storage, pulsed power supply, energy storage, pyroelectric effect

1. Introduction

$(Bi_{0.5}Na_{0.5})TiO_3$ (BNT) was first reported by Smolenskii et al. in 1960 [1]. BNT ceramic is a kind of ABO3 type ferroelectrics which is replaced by Na^+ and Bi^{3+} complex ions at A-site. The A-site ions of BNT ceramics are located at the eight corner positions of octahedron, and the B-site ions are at the body center of octahedral structure [2]. Well sintered BNT ceramics have been obtained by hot pressing sintering method with d_{33} of 94–98 pC/N [3]. BNT ceramics exhibit a high Curie temperature (~320°C) and high polarization of 38 μC/cm^2, which is considered to be one of the most promising environment-friendly ceramic system to replace lead-based ceramics [4].

Pure BNT ceramics exhibits some problems such as high conductivity, and large coercive field, consequently giving problems in the poling process [4], which seriously hinder its practical application. Studies show that the comprehensive properties of BNT system can be significantly improved by doping or by incorporation

BNT-based piezoelectric ceramics	d_{33} (pC/N)	Ref.
$(Bi_{1/2}Na_{1/2})TiO_3$	94–98	[3]
$(Bi_{1/2}K_{1/2})TiO_3$	69	[10]
$(1\text{-}x)$ $(Bi_{1/2}Na_{1/2})TiO_3\text{-}x(Bi_{1/2}K_{1/2})TiO_3$	140–192	[11]
$(Na_{1}xK_{x})_{0.5}Bi_{0.5}TiO_3$	192	[12]
$85(Bi_{1/2}Na_{1/2})TiO_3\text{-}12(Bi_{1/2}K_{1/2})TiO_3\text{-}3BaTiO_3$	158	[13]
$(Bi_{0.5}Na_{0.5})TiO_3\text{-}Ba(Zr, Ti)O_3$ + 2 mol% CuO	156	[14]
$BiNaTiO_3\text{-}BiKTiO_3\text{-}BiLiTiO_3$	230	[15]
$[(Bi_{0.98}La_{0.02}Na_{1}xLi_{x})_{0.5}]_{0.94}Ba_{0.06}TiO_3$	212	[16]
$(Bi_{1/2}Na_{1/2})TiO_3\text{-}(Bi_{1/2}K_{1/2})TiO_3\text{-}(Bi_{1/2}Li_{1/2})TiO_3\text{-}BaTiO_3$	163	[17]
$Bi_{0.5}Na_{0.5}TiO_3\text{-}Bi_{0.5}K_{0.5}TiO_3\text{-}Bi_{0.5}Li_{0.5}TiO_3$	147–231	[18]

Table 1.
Piezoelectric properties (d_{33}) of BNT-based ceramics [9].

with other components to form solid solutions. In recent years, investigation of BNT based ceramics mainly focuses on two aspects. On one hand, the phase transformation and structure change of BNT under external field (electric field, temperature and stress field). On the other hand, the properties enhancement of BNT-based were obtained by doping or by incorporation with other components to form solid solutions, such as $Bi_{0.5}Na_{0.5}TiO_3\text{-}BaTiO_3$(BNT-BT) [5], $Bi_{0.5}Na_{0.5}TiO_3\text{-}Bi_{0.5}K_{0.5}TiO_3$(BNT-BKT) [6] and other systems [7, 8] to promote its application in sensors and actuators.

At present, BNT system is mainly about its piezoelectric properties. The piezoelectric properties of well-known BNT-based system were reported in **Table 1** [9]. However, because of its strong ferroelectricity, BNT-based ceramics also exhibit great potential in the fields of energy storage, energy conversion and pyroelectric applications. In this chapter, new bismuth sodium titanate ceramics were synthesized and characterized, the ferroelectric properties, phase transition behaviors under external fields and related applications, such as application in energy storage, energy conversion and pyroelectric detection were proposed.

2. New BNT-based ceramics for energy storage applications

BNT-based materials possess a superior potential for energy storage due to their high saturation polarization which originates from hybridization between the Bi *6p* and O *2p* orbitals. However, the pure BNT materials at room temperature own a ferroelectric perovskite structure with the polar *R3c* space group, usually exhibiting a saturated polarization loop with high remnant polarization, which is very unfavorable to obtain good energy storage performance [19]. Fortunately, the BNT materials can show an antiferroelectric-like behavior at around 200–320°C, which opens a door to the energy storage application of BNT-based materials, and the 200°C is identified as the depolarization temperature (T_d) of the BNT materials, which correspond with a peak in the temperature-dependent dielectric loss curve. The structure at this temperature range is still under debate. Zvirgzds et al. [20] proposed a rhombohedral (*R3c*)-tetragonal (non-polar *P4bm*) phase transition over the broad temperature range (255–400°C). Moreover, Schmitt et al. [21] suggested the phase transformation from non-polar *P4bm* phase to polar *R3c* phase under applied electric field

accounted for the antiferroelectric-like characteristic, but this could not reasonably explain a large temperature hysteresis of different physical properties about the phase transition between 200 and 320°C. Dorcet et al. [22] revealed a modulated phase at 200–300°C through in-situ Transmission electron microscope (TEM) characterization, it was formed of *Pnma* orthorhombic sheets which are locally analogous to an antiferroelectric phase, and these sheets are twin boundaries between *R3c* ferroelectric domains. The phase structure evolution disclosed by Zvirgzds et al. [21] well matches the macroscopic physical properties of BNT materials during the heating process.

In 1947, Sakata et al. reported an antiferroelectric-like behavior in the 0.85BNT-0.15$SrTiO_3$ ceramics [23]. Later, Zhang et al. introduced (K, Na)NbO_3 (KNN) into BNT-$BaTiO_3$ (BT) ceramics to low the phase transition temperature and achieved the antiferroelectric-like behavior in BNT-BT-KNN ceramics with slanted polarization hysteresis loops at room temperature [24]. In 2011, Gao et al. [25] first investigated the energy storage properties of the BNT-BT-KNN system, the 0.89BNT-0.06BT-0.05KNN ceramics was chosen as the object, **Figure 1(a)** is the temperature-dependent dielectric properties of the 0.89BNT-0.06BT-0.05KNN ceramics, it can be seen that these ceramics showed much lower T_d compared with pure BNT materials, indicating the antiferroelectric-like behavior at a lower temperature. **Figure 1(b, c)**show the temperature dependence of polarization hysteresis loops of the 0.89BNT-0.06BT-0.05KNN ceramics under different electric fields. At 20°C, the polarization hysteresis loop was more of ferroelectric featured with coercive field E_c = 0.9 kV/mm and remnant polarization P_r = 6.2 μC/cm^2 under 6 kV/mm. At 110°C, the polarization hysteresis loop was more of an antiferroelectric-like feature with a pronounced shrinkage in both E_c and P_r compared with those at 20°C. The energy density as a function of the temperature of the 0.89BNT-0.06BT-0.05KNN ceramics are displayed in **Figure 1(d)**. An energy density of

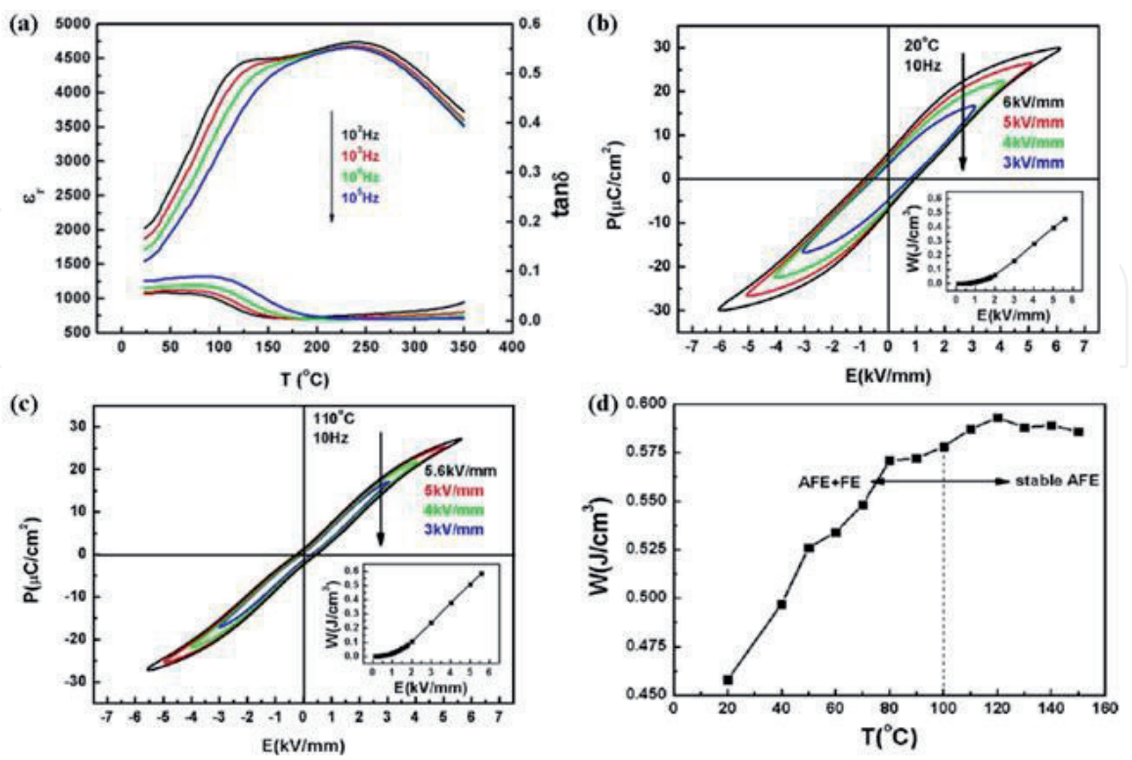

Figure 1.
Properties of 0.89BNT-0.06BT-0.05KNN ceramics: (a) the temperature-dependence of dielectric properties, (b) the polarization-electric field (P-E) loops at 20°C, (c) the P-E loops at 110°C, (d) the energy density as function of temperature [25].

around 0.59 J/cm^3 under 5.6 kV/mm at 10 Hz was obtained in 0.89BNT-0.06BT-0.05KNN ceramics from 100 °C to 150 °C, indicating high stability of temperature in the antiferroelectric-like region. Although the obtained energy density was very small and only existed above 100°C, this work is still meaningful because it inspires the further way for studying energy-storage in BNT-based materials. After, researches about the energy storage properties in BNT-based ceramics have been extensively reported.

Ren et al. [26] reported that the introduction of KNN would decrease the T_d of BNT-$BiAlO_3$ (BA) ceramics and the KNN content exerts a significant influence on the polarization hysteresis loops of BNT-BA-KNN materials as shown in **Figure 2b**. For 0.93 (0.96BNT-0.04BA)-0.07KNN ceramics, the T_d was below the room temperature as depicted in **Figure 2a** and these ceramics were more of antiferroelectric-like behavior. Ren et al. [26] also investigated the energy storage properties of 0.93 (0.96BNT-0.04BA)-0.07KNN ceramics, an energy storage density of 0.65 J/cm^3 was obtained under 8 kV/mm at room temperature, and these ceramics exhibited good stability of energy density as a function of temperature and frequency at 7 kV/mm, which can be seen from **Figure 2c**,**d**.

Due to the high energy loss of the antiferroelectric-like BNT-based materials, the BNT-based relaxor ferroelectrics have attracted more and more attention for energy storage and usually can show superior energy storage performance. In fact, by modifying composition and temperature in BNT-based systems, a normal or square P-E loop can transform into a slim P-E loop due to the occurring of an ergodic relaxor phase, which can be contributed to the energy storage properties. Wu et al. [27] focused on the energy storage characteristics of BNT-based relaxor ferroelectric ceramics and introduced $Sr_{0.85}Bi_{0.1}\square_{0.05}TiO_3$ (□ represents the A site vacancy) and $NaNbO_3$ into the BNT matrix as illustrated in **Figure 3**. The introduced A site

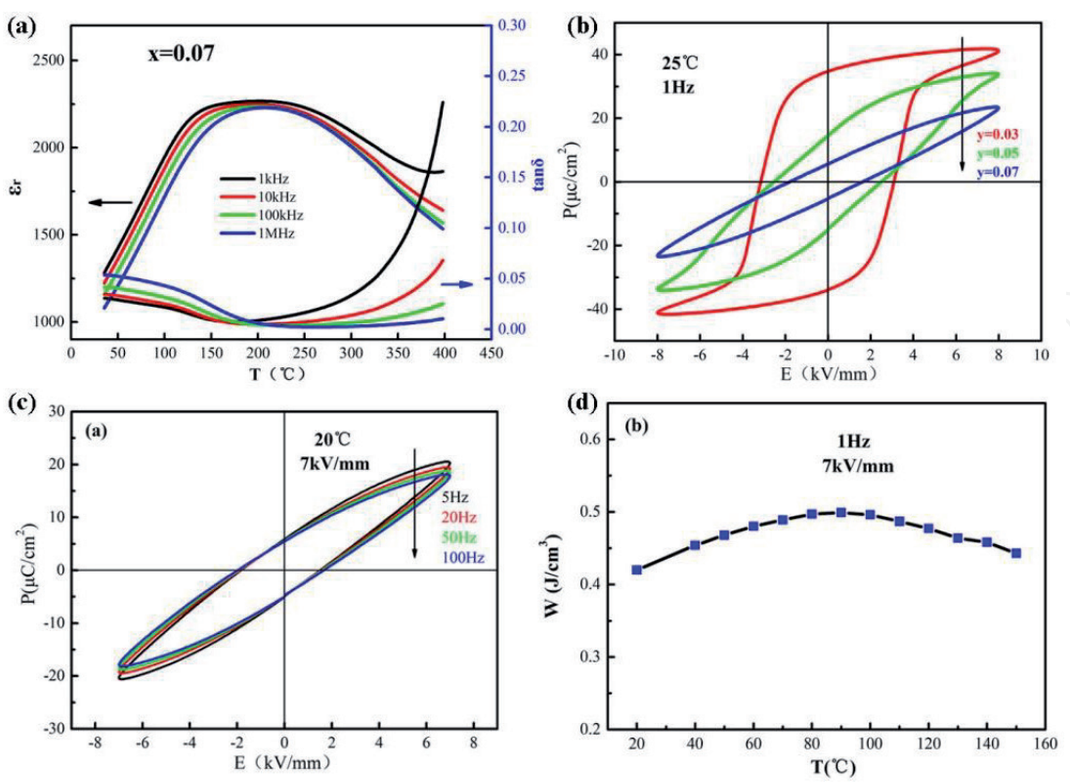

Figure 2.
(a) The temperature dependence dielectric properties of the 0.93 (0.96BNT-0.04BA)-0.07KNN ceramics. (b) The P-E loops of the (1-x)(0.96BNT-0.04BA)-xKNN ceramics. (c) The P-E loops of the 0.93 (0.96BNT-0.04BA)-0.07KNN ceramics under different frequencies. (d) The energy density of 0.93 (0.96BNT-0.04BA)-0.07KNN ceramics at different temperatures [26].

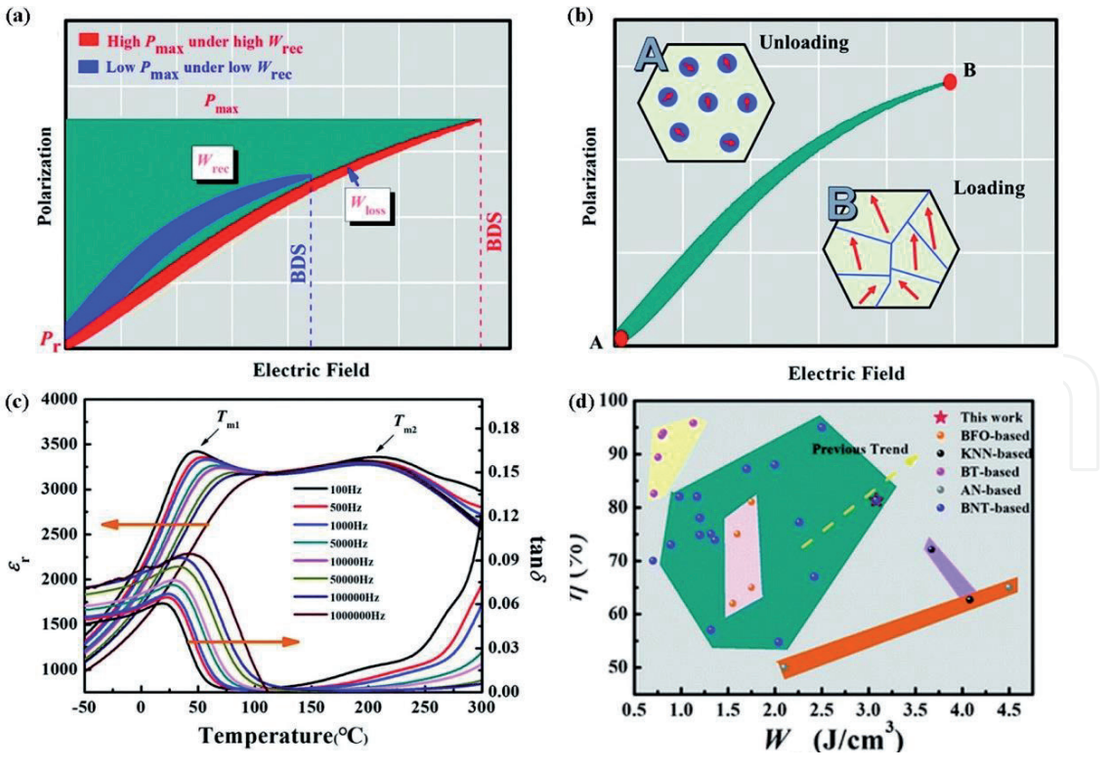

Figure 3.
(a) Schematic image showing energy storage properties under different electric fields. (b) Schematic image showing polar structure in relaxor ferroelectrics under loading and unloading electric fields. (c) The dielectric permittivity and loss as a function of temperature, measured at different frequencies from 0.1 kHz to 1 MHz for the 0.96 ($0.65Bi_{0.5}Na_{0.5}TiO_3$–$0.35Sr_{0.85}Bi_{0.1}TiO_3$)–$0.04NaNbO_3$ ceramics. (d) Energy efficiency versus recoverable energy density value for the 0.96 ($0.65Bi_{0.5}Na_{0.5}TiO_3$–$0.35Sr_{0.85}Bi_{0.1}TiO_3$)–$0.04NaNbO_3$ ceramics compared to other lead-free systems [27].

vacancy and Sr^{2+}, Nb^{5+} ions replaced the A- and B- sites ions respectively, which led to the stress mismatch and charge imbalance. These effects acted together to effectively form a local random field, which broke the long-range ordered structure of the dipole in the matrix and formed a weakly coupled polar nanodomain. Under the applied electric field, the modified ceramics exhibited a small hysteresis and a small remnant polarization, achieving high energy storage density (3.08/cm^3) and high energy storage efficiency (81.4%). To evaluate the practicability of the modified ceramic, energy storage performance test in a wide range of temperature and frequency found that the variations of its energy storage performance at RT ~ 100°C and 1 Hz ~ 100 Hz was less than 10%. The modified ceramics with excellent application prospects are excellent candidate materials for dielectric energy storage capacitors.

3. New BNT-based ceramics for pulse power supply application

Ferroelectric materials have an important application in pulse power supply due to their shock compression induced depolarization behavior [28]. At present, the main material systems studied are PZT52/48 piezoelectric ceramics [28], PZT95/5 ceramics [28, 29] and PIN-PMN-PT single crystals [30]. However, due to the toxicity of Lead, it is urgent to develop lead-free materials for high ferroelectric pulse power supply.

$Bi_{0.5}$ $Na_{0.5}TiO_3$ (BNT) is explored as an alternative lead-free candidate for pulse power supply, in view of its high P_r, high breakdown strength E_b, low bulk density, and relatively high Curie temperature (T_c). Gao et al. [31] reported that the BNT

can be fully depolarized by shock compression and generate a giant power output (3.04×10^8 W/kg). This power output is mainly attributed to a two-step polar-nonpolar phase transition from rhombohedral to orthorhombic under shock pressure.

Figure 4 shows that BNT is polar phase and rhombohedral (space group R3c) at low pressure, and transforms via a first-order phase transition to a nonpolar phase (space group Pnma), which is orthorhombic and centrosymmetric. The electrical output of BNT from depoling under shock compression can be attributed to the ferroelectric-to-paraelectric (R3c – Pnma) phase transition. The energy output under shock compression in BNT is larger than that reported in other ferroelectric materials, mainly due to a first-order R-O phase transition under high dynamic pressure. This phase transition undergoes two steps, which correspond to the unit-cell shrinkage and O^{2-} ions chain rearrangement, respectively, as shown in **Figure 5**. These results will extend the potential application of the pressure induced depolarization effects and guide the application and development of BNT ferroelectric materials.

Liu et al. [32] report the pressure driven depolarization behavior in 0.97[(1-x) $Bi_{0.5}Na_{0.5}TiO_3$-x $BiAlO_3$]-0.03$K_{0.5}Na_{0.5}NbO_3$ (BNT-xBA-0.03KNN) ceramics. Particularly, with increasing hydrostatic pressure from 0 MPa to 495 MPa, the polarization of BNT-0.04 decreases from 30.7 μC/cm^2 to 8.2 μC/cm^2, decreasing ~73%. The observed depolarization effect is associated with the pressure induced polar ferroelectric -nonpolar relaxor phase transition. The results revealed that BNT-xBA-0.03KNN ceramics as promising lead-free candidates for energy conversion applications based on the pressure driven depolarization effect.

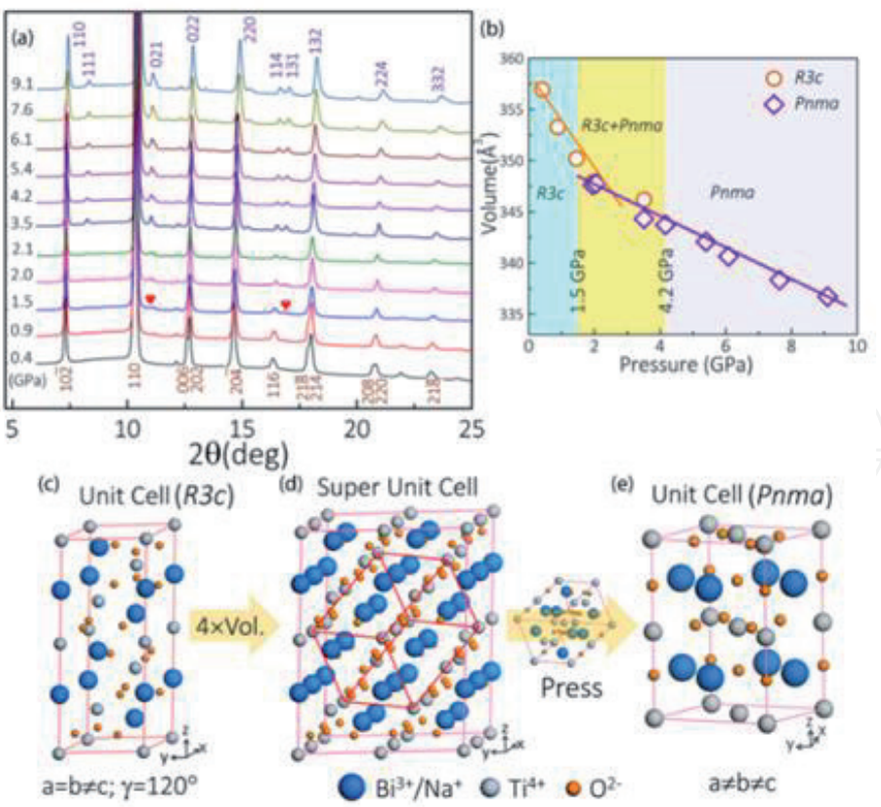

Figure 4.
Pressure dependence of the phase transition in BNT has been studied by the in situ synchrotron x-ray diffraction [31]. (a) The x-ray diffraction spectra of NBT ferroelectric materials at selected pressures. (b) The XRD peaks of the phase are marked by the red spades. The NBT is rhombohedral (R3c) structure at low pressure, and it changes into orthorhombic structure (Pnma) at high pressure. The normalized P-V curve of NBT according to the Z = 6, and (c)–(e) the schematic diagram of the structure phase transition during the phase transition.

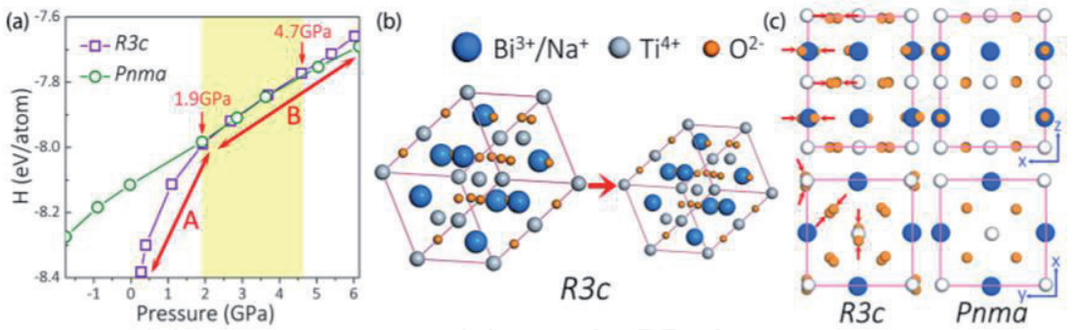

Figure 5.
First-principles calculations of the R3c and Pnma phases as a function of pressure [31]. (a) The enthalpy (H) calculated by first-principles simulation for R3c and Pnma phases at different pressures, respectively. The enthalpy change of R3c phase could be divided into two regions (A and B). When the pressure is below 1.9 GPa (region A), the enthalpy of R3c increases sharply due to the volume decreasing as shown in (b). When the pressure is above 1.9 GPa (region B), the enthalpy of R3c phase increases gently, which is mainly due to the O2−ions displacing following the red arrows in (c).

Figures 6 and 7 show the effect of hydrostatic pressure on the ferroelectric properties of BNT-0.01BA-0.03KNN and BNT-0.04BA-0.03KNN, respectively. It is clear that the P_r and P_m decrease monotonically with increasing pressures, which further confirms the increasing the instability of the long-range FE order and the energy barrier for the formation of FE domains under hydrostatic pressure conditions. In addition, the response of BNT-0.04BA-0.03KNN under pressure is more sensitive than that of BNT-0.01BA-0.03KNN. And the thermally induced depolarization is also stronger for BNT-0.04BA-0.03KNN. These phenomena should be related to their different depolarized temperature values. The ER phase exhibits smaller volume than the FE phase. Therefore, applying compressive pressure favors

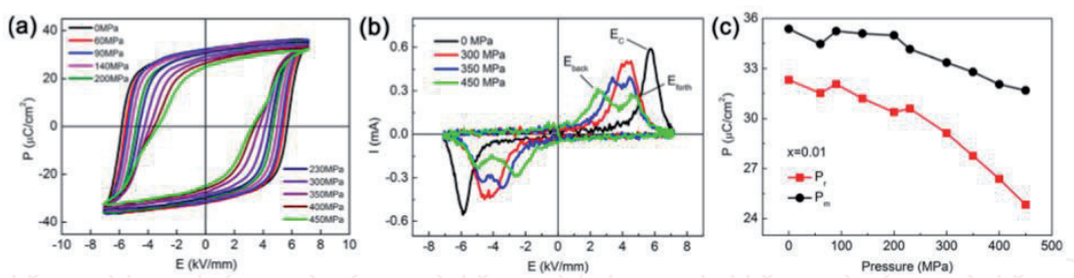

Figure 6.
(a) P-E loops and (b) I-E curves of BNT-0.01BA-0.03KNN ceramics under different hydrostatic pressures; and (c) the pressure dependence of maximum polarization and remanent polarization of BNT-0.01BA-0.03KNN ceramics [32].

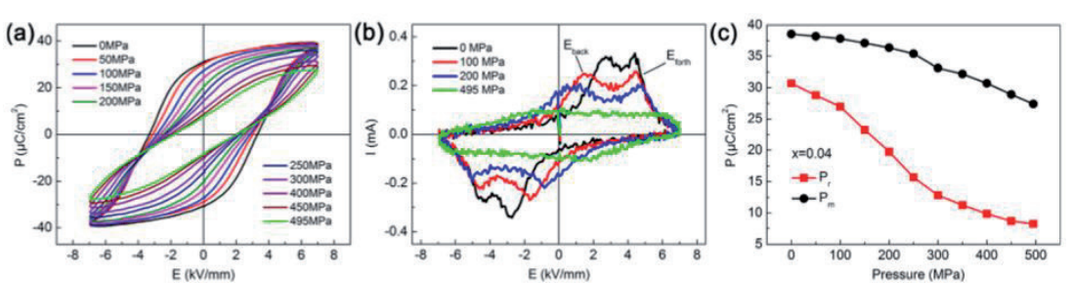

Figure 7.
(a) P-E loops and (b) I-E curves of BNT-0.04BA-0.03KNN ceramics under different hydrostatic pressures; (c) the pressure dependence of maximum polarization and remanent polarization of BNT-0.04BA-0.03KNN ceramics [32].

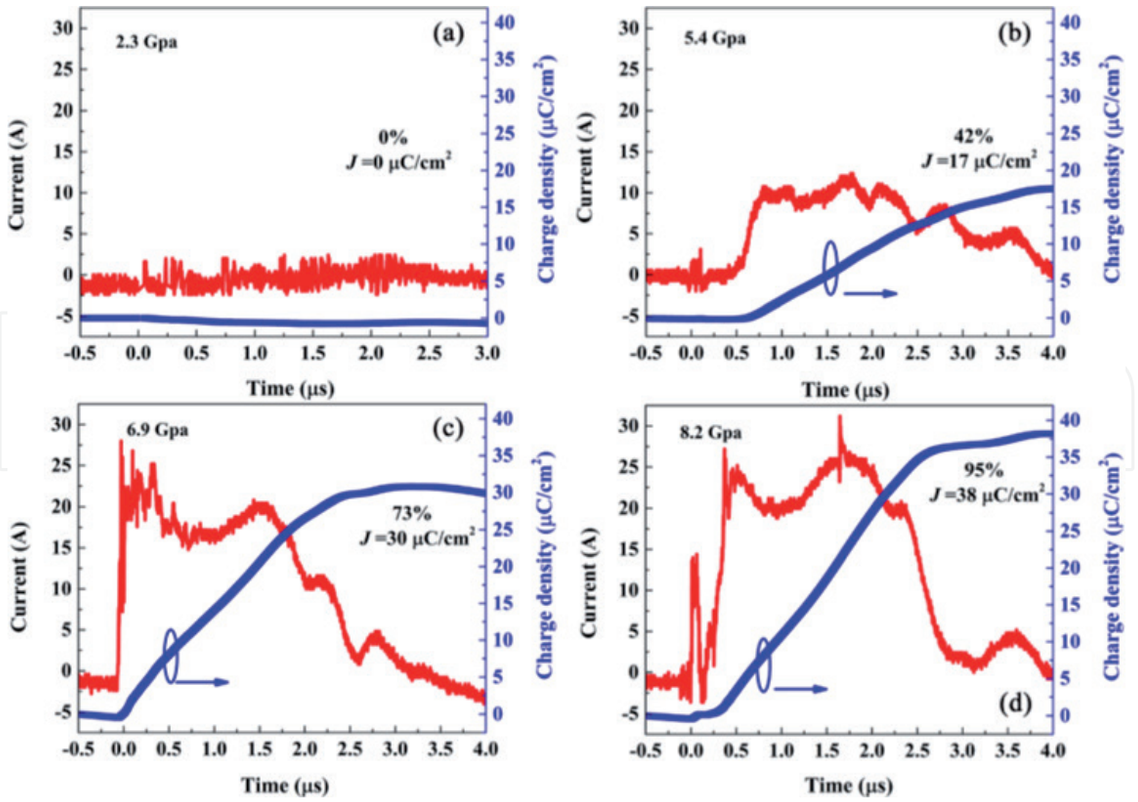

Figure 8.
Dynamic response behaviors of BNT-BA-0.01NN ceramics in a short-circuit mode under different shock pressures [34]. (a) 2.3 GPa, (b) 5.4 GPa, (c) 6.9 GPa, (d) 8.2 GPa.

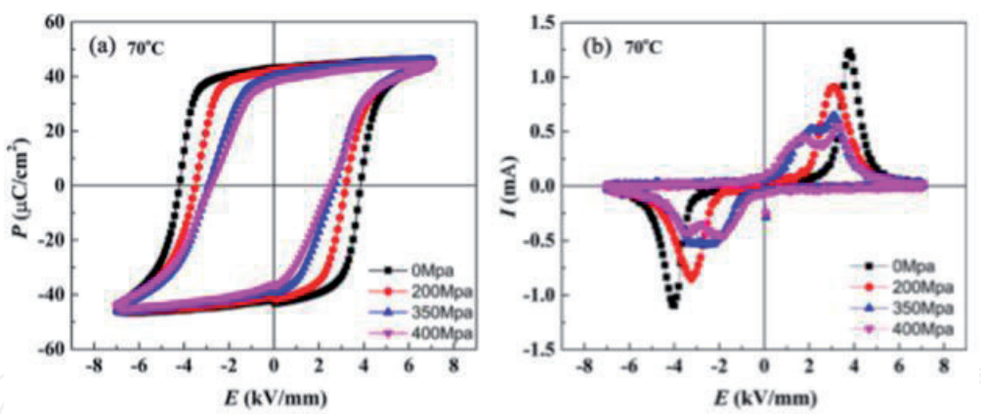

Figure 9.
Pressure-dependent (a) P-E and (b) I-E loops of unpoled BNT-BA-0.01NN ceramics at 70°C [34].

the FE-ER phase transition. This is quite similar to the case of Nb doped PZT95/5, in which pressure can drive the larger volume FE phase to transform into the smaller volume AFE phase.

Peng et al. [33, 34] report the depolarization behavior of lead-free ternary $0.99[0.98\ (Bi_{0.5}Na_{0.5})(Ti_{0.995}Mn_{0.005})\ O_3–0.02BiAlO_3]$-$0.01NaNbO_3$ (BNT-BA-0.01NN) ferroelectric ceramics under shock wave compression. Particularly, approximately complete depolarization under shock compression was observed in the poled BNT-BA-0.01NN ceramics, releasing a high discharge density J of 38 μC/cm^2. The released J was 96% of thermal-induced discharge density (~40 μC/cm^2). This discharge density J was 18% higher than that of PZT95/5 ceramics [29]. The shock-induced depolarization mechanism can be attributed to the ferroelectric-ergodic relaxor phase transition. These results reveal the BNT-based ceramics as promising candidates for pulsed power applications.

Figure 8 shows the BNT-based ceramics were almost completely depolarized, similar to PZT95/5 ceramics [29] and PIN-PMN-PT crystals [30], which indicate a similar depolarization mechanism, that is, a stress-induced phase transition. Although the released J in BNT-based ceramics is 26% lower than that obtained in PIN-PMN-PT crystals, the simple preparation methods together with environmental friendliness will be a benefit to their applications in the future. **Figure 9** unveils the possible shock-induced depolarization mechanism of BNT-BA-0.01NN ceramics. The pinched P-E loops gradually emerge and the sharp current peak splits into four peaks, indicating a pressure-induced FE-ER phase transition. It is suggested that applying compressive pressure favors the formation of the ER phase for its smaller volume.

4. New BNT-based ceramics for pyroelectric applications

At present, the most widely used intrinsic pyroelectric materials are perovskite-type lead-containing materials, such as $Pb(Zr, Ti)O_3$ (PZT), $PbTiO_3$ doped with Ca (PCT), $xPb(Mg_{1/3}Nb_{2/3})O_3$-$(1-x)PbTiO_3$ (PMN-PT) [35–40]. Over the last few decades, continuous efforts have been devoted to the development of lead-free pyroelectric ceramics. Many lead-free ceramics such as $Sr_{0.3}Ba_{0.7}Nb_2O_6$-based, $(Ba, Ca)TiO_3$-based, $CaBi_4Ti_4O_{15}$-based bismuth layer-structured and $Bi_{0.5}Na_{0.5}TiO_3$-based ceramics have been investigated [41–44]. Among them, BNT-based ceramics have been regarded as one of most promising alternative lead-free ceramics due to its high pyroelectric coefficient (p), high remnant polarization P_r (around 38μC/cm^2), high Curie temperature T_c (around 320°C), low-cost, and simple synthesis process. In recent decades, pyroelectric properties of BNT-based materials, including pyroelectric coefficient and detection rate, have been greatly improved. The pyroelectric coefficient of BNT-based lead-free pyroelectric materials has been comparable to commercial PZT [45–47]. However, the enhanced pyroelectric property is usually at the cost of degraded depolarization temperature (<150°C) and thermal stability, which are the hurdles to application. The BNT-based pyroelectric ceramics with low Td will depolarize partially or completely during the heat treatment (typically >100°C) processes, causing degradation of pyroelectric performance. Therefore, from the viewpoint of practical application, it is urgent for BNT-based materials to optimize their depolarization temperature, thermal stability and pyroelectric performance, thus further to promote their applications in infrared detection [48, 49].

4.1 BNT- BNN pyroelectric ceramics

$(1-x)(Bi_{0.5}Na_{0.5})TiO_3$-$xBa(Ni_{0.5}Nb_{0.5})O_3$ lead-free pyroelectric ceramics (abbreviated as (1-x)BNT-xBNN) were synthesized by a conventional solid-state reaction method [50], and the thermal stability and depolarization temperature is enhanced at the same time as the excellent pyroelectric performance is maintained. BNN is a compound with a mixed valence state at the b position, which can be solid-solved with BNT and expand a wide range of composition adjustment. The (1-x) BNT-xBNN take into account the advantages of b-position acceptor substitution and donor substitution. The effect of BNN content on phase structure, electrical properties and thermal stability was systematically studied. After the solid-state reaction of BNN, (1-x)BNT-xBNN exhibits enhanced pyroelectric performance with a high depolarization temperature. In addition, it can be exposed to temperature up to ~145°C with negligible deterioration of pyroelectric properties, showing excellent thermal stability.

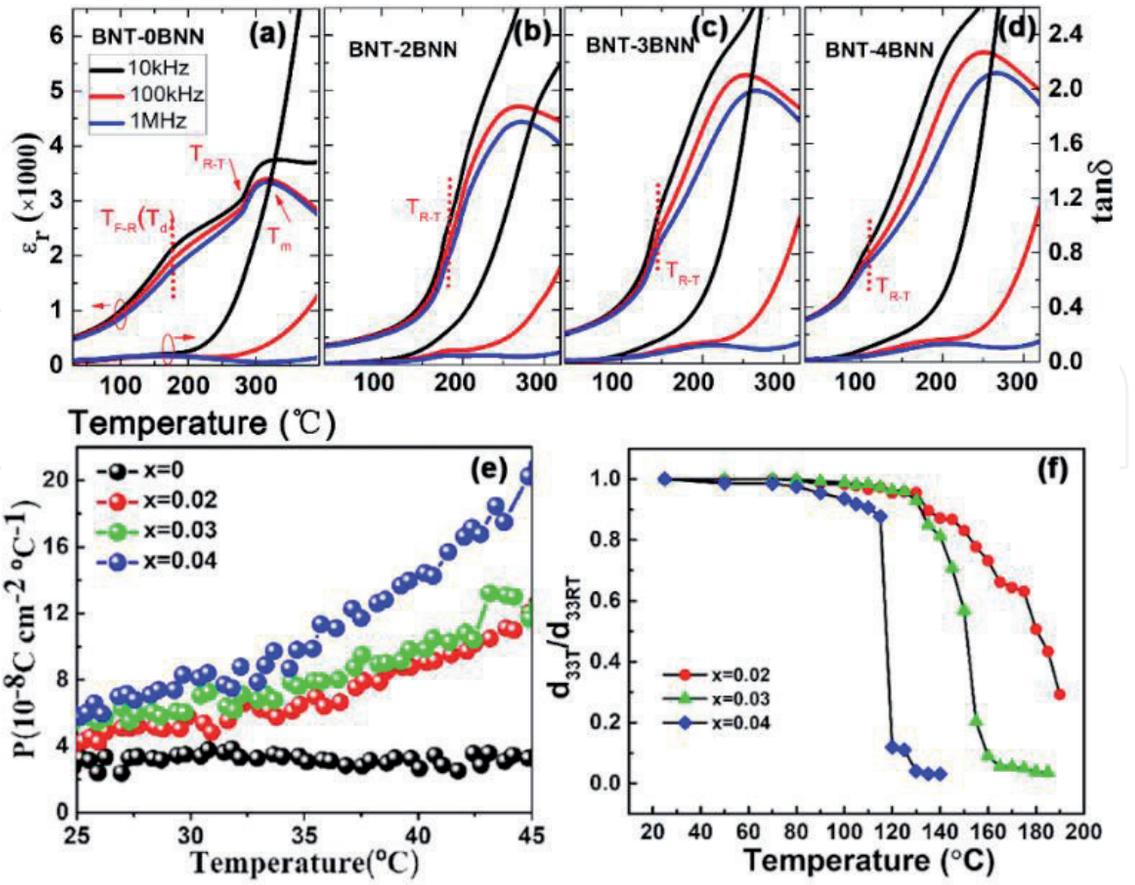

Figure 10.
Temperature dependence of dielectric constant (εr) and dielectric loss (tan δ) for poled (1-x)BNT-xBNN (a) x = 0, (b) x = 0.02, (c) x = 0.03, (d) x = 0.04 in frequency range between 10 kHz and 1 MHz; (e) Pyroelectric coefficient (p) of poled (1-x)BNT-xBNN ceramics as a function of temperature; (f) d33RT/d33T at room temperature after annealing at T_a [50].

The temperature-dependent properties of poled (1 – x)BNT-xBNN ceramics are displayed in **Figure 10a–d**. With the increasing BNN content, the Curie temperature Tc indicated by the maximum dielectric constant decreases and dielectric constant and dielectric loss of BNN decrease first and then increase. The minimum value of dielectric constant and dielectric loss occurs when the BNN content is 2%, which further improve the pyroelectric detection rate figure of merit. The depolarization temperature T_d can be characterized by the first anomal point of temperature dependent dielectric properties, and the content of 2% has the highest depolarization temperature. As shown in **Figure 10e**, after the increase of BNN, the room temperature p values rise from 3.01 × 10^{-8}C/cm^{2}K of pure BNT to 5.94 × 10^{-8}C/cm^{2}K of 0.96BNT-0.04BNN with the increasing addition of BNN, which gains advantage compared with many other lead-free ceramics. The *p* value of (1-x)BNT-xBNN ceramics increases sharply, which indicates that the (1-x)BNT-xBNN sample is sensitive to ambient temperature. In addition, it can be seen that the p value increases with the increasing temperature, which indicates that the (1 – x)BNT-xBNN samples are sensitive to the surrounding temperature. Besides, 0.98BNT-0.02BNN ceramics have the best thermal stability and it can withstand heat treatment at 145°C without depolarization (**Figure 10f**), which is attributed to the domain switching and phase transition.

4.2 BNT-BT pyroelectric ceramics

BNT-BT possesses a rich phase structure, which can be easily adjusted by varying the BT content. Because of the low tripartite-tetragonal transition barrier, the

morphotropic phase boundary (MPB) of BNT-BT, located at where the BT content is approximately 6%, exhibits the best pyroelectric properties and has received much attention. But it is not advisable to blindly pursue a high pyroelectric coefficient. The improvement of pyroelectric performance is often at the cost of low depolarization temperature, which is not helpful to practical applications. However, it is found that the sample with high BT content is in the tetragonal phase, which brings a higher T_d than that of the tripartite, but there is no relevant report on the pyroelectric performance of high BT content.

Based on the above ideas, the tetragonal phase 0.8BNT-0.2BT lead-free pyroelectric material with high BT content was successfully prepared, and the microstructure, dielectric properties, pyroelectric properties, and thermal stability were studied [51]. Owing to its high T_d, this composition can endure high-temperature environment (180°C) for half hour with the value of p at room temperature remains ~90% of its initial value, demonstrating that the 0.8BNT-0.2BT samples show excellent thermal stability. Moreover, the T_d of the samples is up to ~209°C, which is far higher than that of the reported BNT-based, pyroelectric materials, and it is also comparable to the commercial PZT materials.

The pyroelectric properties of 0.8BNT-0.2BT pyroelectric ceramics between 25 and 70°C are investigated. With the increase of temperature, the pyroelectric performance shows an increasing trend, indicating that the material has good pyroelectric performance in a wide temperature range. Meanwhile, because the 0.8BNT-0.2BT sample has a low dielectric constant and dielectric loss, it will show a larger detection merit (**Figure 11a**). In order to study the depolarization temperature of the material, the dielectric thermo diagram of the sample was shown in **Figure 11b**. When the temperature rises to about 209°C, the dielectric constant of the sample suddenly increases with a dielectric loss peak appearing, indicating that this temperature is the

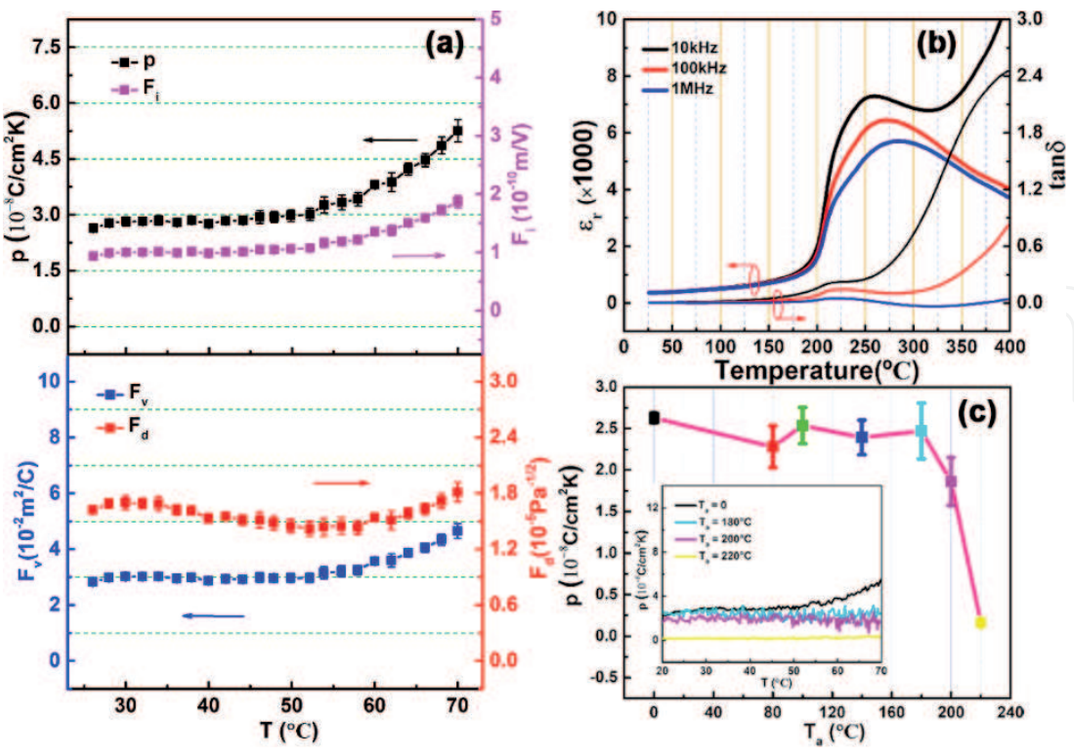

Figure 11.
(a) Pyroelectric coefficient (p) and figures of merit (F_i, F_v, F_d) as a function of temperature on heating during the range of RT to 70°C. The figures of merit are determined based on the values of p, C_V, ε_r, and tanδ; (b) temperature-dependent dielectric constant (ε_r) and dielectric loss (tanδ) of poled 0.8BNT–0.2BT ceramics; (c) pyroelectric coefficient at room temperature after annealing at Ta. The inset shows the temperature-dependent pyroelectric coefficient on heating after annealing at Ta [51].

depolarization temperature T_d. Notably, the depolarization temperature of reported BNT-based pyroelectric materials is generally lower than 180°C. The materials with high Td (209°C) and high pyroelectric coefficient discovered lay the foundation for the further development of lead-free pyroelectric materials. Moreover, it can be observed from **Figure 11c** that the room temperature pyroelectric coefficient of 0.8BNT-0.2BT maintains about 90% of the original data after being treated at 180°C, indicating that the material has good temperature stability and can withstand high temperature treatment up to180°C without pyroelectric performance loss.

4.3 BNT-BA-NN pyroelectric ceramics

A new ternary system 0.98BNT-0.02BA-xNN ceramic was obtained by solid solution of $NaNbO_3$ (NN) in the BNT-BA system and Mn element substitution

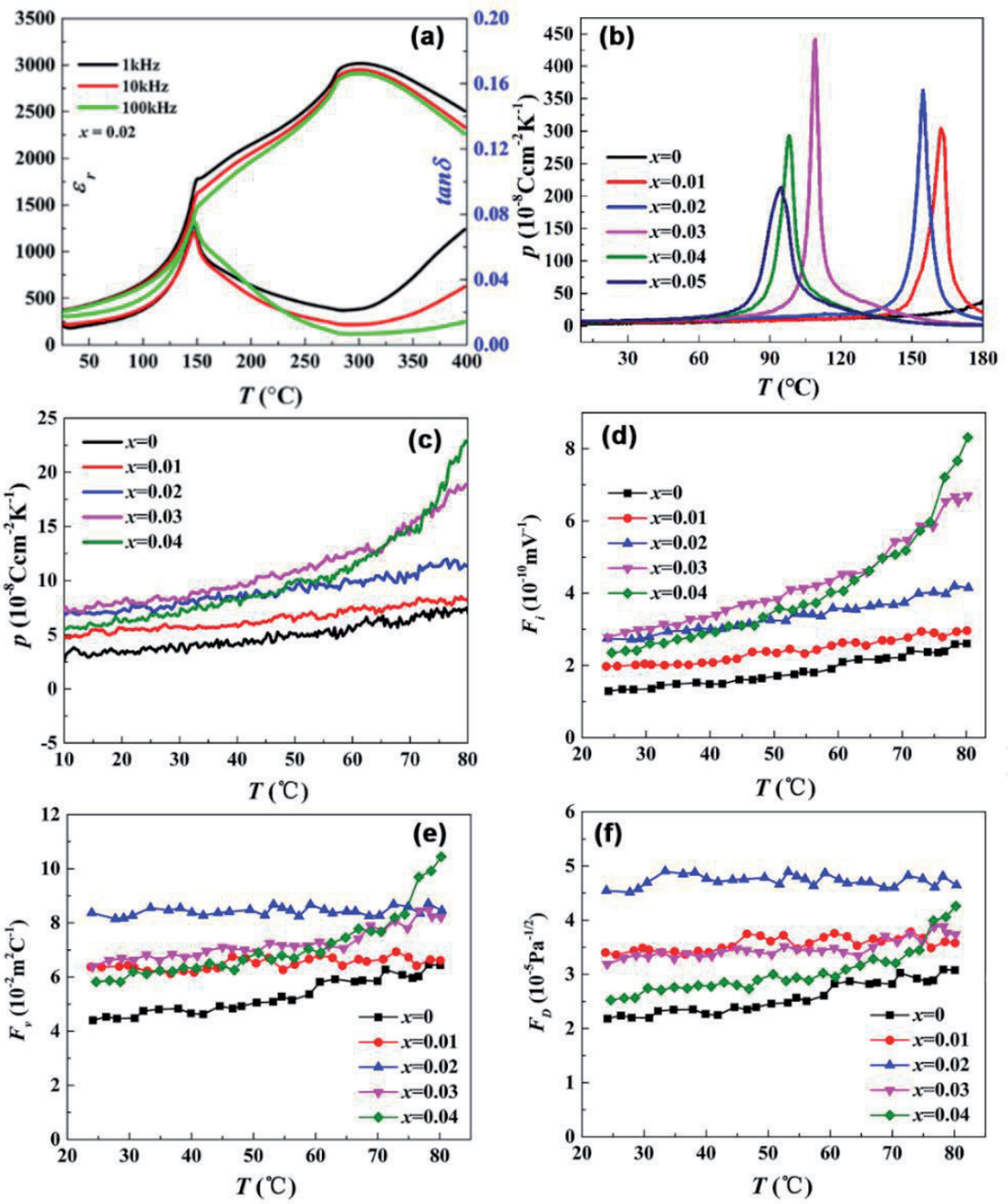

Figure 12.
(a) Temperature dependent dielectric constant (ε_r) and tangent loss (tanδ) of 0.98BNT-0.02BA-xNN ceramics; (b) temperature-dependent pyroelectric coefficient of 0.98BNT-0.02BA-xNN ceramics; (c) the temperature-dependent pyroelectric coefficient p of 0.98BNT-0.02BA-xNN ceramics in the temperature range from 10–80°C; merit (d) F_i, (e) F_v and (f) F_d of 0.98BNT-0.02BA-xNN ceramics measured at 1 kHz over the range of 20–80°C [52].

modification [52]. The NN solution significantly affect the microstructure, phase transition and pyroelectric properties of 0.98BNT-0.02BA-*x*NN ceramics. It was found that NN addition tends to reduce the rhombohedral phase while favoring the formation of the tetragonal phase. The compositions exhibit excellent pyroelectric performance. All components exhibit excellent ferroelectric properties at room temperature, and the Pr values are all higher than 35 μC/cm^2, of which the Pr of the x = 0.03 component is the largest, reaching 45 μC/cm^2.

Furthermore, the influence of NN solid solution on the relaxation characteristics and phase transition of BNT-BA-based ceramics was analyzed by testing the temperature-changing dielectric properties in **Figure 12a**. **Figure 12b** shows the change curve of the pyroelectric coefficient of 0.98BNT-0.02BA-xNN after polarization with temperature changing. The FE-RE phase transition occurs at T_d, corresponding to the sudden drop in the polarization intensity P_r. the largest peak appears at the composition x = 0.03, reaching 441.0 × 10^{-8} C/cm^{2}K, which is much larger than other BNT-based ceramics reported. As the NN content increases, the T_d continuously decreases. Notably, t the T_d of the x = 0.02 component is still as high as 155°C. It can be observed from **Figure 12c** that the introduction of NN significantly improves the room temperature pyroelectric coefficient. With the increase of NN content, the p under room temperature (25°C) first increases and then decreases, and the maximum value is obtained at x = 0.03 (p = 8.45 × 10^{-8} C/cm^{2}K), which improved about 54% compared to the matrix (x = 0, p = 3.87 × 10^{-8} C/cm^{2}K). Moreover, the optimal figure of merit (FOMs) at room temperature were obtained at x = 0.02 with F_i = 2.66 × 10^{-10} m/V, F_v = 8.07 × 10^{-2} m^2/C, and F_d = 4.22 × 10^{-5} Pa$^{-1/2}$ (**Figure 12d–f**). Furthermore, the compositions with $x \leq 0.02$ possess relatively high depolarization temperature (≥155°C). Those results unveil the potential of 0.98BNT-0.02BA-*x*NN ceramics for infrared detector applications.

5. Conclusion

Due to its strong ferroelectric properties, BNT-based ceramics exhibit great potential in the fields of energy storage, pulsed power supply and pyroelectric applications. In this chapter, new bismuth sodium titanate ceramics were synthesized and characterized via composition modifications, the ferroelectric properties, phase transition behaviors under external fields and related applications were proposed in this chapter. To detail, BNT-BT-KNN, BNT-BA-KNN, and BNT-SBT-NN ceramics for energy storage application, BNT, BNT-BA-KNN, and BNT-BA-NN ceramics for pulsed power supply, as well as BNT-BNN, BNT-BT, and BNT-BA-NN for pyroelectric detection application were presented.

Acknowledgements

The authors would like to thank the financial support by Youth Innovation Promotion Association, CAS (Grant No. 2017296), National Natural Science Foundation of China (NSFC) (Grant No. 51872312), and Natural Science Foundation of Shanghai (Grant NO.18ZR1444900).

Conflict of interest

The authors declare no conflict of interest.

Author details

Hengchang Nie[1], Genshui Wang[1,2,3] and Xianlin Dong[1,2,3]*

1 Key Laboratory of Inorganic Functional Materials and Devices, Shanghai Institute of Ceramics, Chinese Academy of Sciences, Shanghai, China

2 Hangzhou Institute for Advanced Study, UCAS, Hangzhou, China

3 Center of Materials Science and Optoelectronics Engineering, University of Chinese Academy of Sciences, Beijing, China

*Address all correspondence to: xldong@mail.sic.ac.cn

References

[1] GA Smolenskii, VA Isupov, AI Agranovskaya, NN Krainik. Ferroelectrics with diffuse phase transition. Soviet Physics Solid State. 1961;2:2651. (doi is not available)

[2] YM Li, W Chen, Q Xu, J Zhou, HJ Sun, R Xu. Dielectric and piezoelectric properties of lead-free $(Na_{0.5}Bi_{0.5})TiO_3$-$NaNbO_3$ ceramics. Materials Science & Engineering B. 2004;112:5-9. DOI:10.1016/j.mseb.2004.04.019.

[3] H Nagata, T Shinya, Y Hiruma, T Takenaka. Developments in Dielectric Materials and Electronic Devices, Ceramic Transactions. 2004;167:213-221.

[4] PK Panda. Review: environmental friendly lead-free piezoelectric materials, Journal of Materials Science. 2009;44:5049-5062. DOI: 10.1007/s10853-009-3643-0.

[5] T Takenaka, K Maruyama, K Sakata. $(Bi_{1/2}Na_{1/2})TiO_3$-$BaTiO_3$ system for lead-free piezoelectric ceramics. Japanese Journal of Applied Physics. Part 1, 1991;30: 2236-2239. DOI: 10.1143/JJAP.30.2236.

[6] J Rödel, W Jo, K Seifert, EM Anton, T Granzow, D Damjanovic. Perspective on the development of lead-free piezoceramics. Journal of American Ceramic Society. 2009;92:1153-1177. DOI: 10.1111/j.1551-2916.2009.03061.x.

[7] CR Zhou, XY Liu. Dielectric and piezoelectric properties of bismuth-containing complex perovskite solid solution of $Bi_{1/2}Na_{1/2}TiO_3$-$Bi(Mg_{2/3}Nb_{1/3})O_3$. Journal of Materials Science. 2008;43:1016. DOI:10.1007/s10853-007-2246-x.

[8] S Mahboob, G Prasad, GS Kumar. Impedance spectroscopy and conductivity studies on B site modified $(Na_{0.5}Bi_{0.5})(Nd_xTi_{1-2x}Nb_x)O_3$ ceramics. Journal of Materials Science. 2007; 42:10275. DOI:10.1007/s10853-006-1122-4.

[9] P. K. Panda & B. Sahoo, PZT to Lead Free Piezo Ceramics: A Review, Ferroelectrics, 2015; 474:1, 128-143, DOI: 10.1080/00150193.2015.997146.

[10] Y Hiruma, R Aoyagi, H Nagata, T Takenaka, Ferroelectric and Piezoelectric Properties of $(Bi_{1/2}K_{1/2})TiO_3$ Ceramics. Japanese Journal of Applied Physics. Part 1, 2005; 44: 5040-5044. DOI: 10.1143/JJAP.44.5040.

[11] Z Yang, B Liu, L Wei, Y Hou. Structure and Electrical Properties of $(1-x)Bi_{0.5}Na_{0.5}TiO_3$–$xBi_{0.5}K_{0.5}TiO_3$ Ceramics Near Morphotropic Phase Boundary. Materials Research Bulletin. 2008;43:81-89. DOI: 10.1016/j.materresbull.2007.02.016.

[12] YR Zhang, JF Li, BP Zhang, Enhancing Electrical Properties in NBT–KBT Lead-Free Piezoelectric Ceramics by Optimizing Sintering Temperature, Journal of the American Ceramic Society. 2008;91:2716-2719. DOI: 10.1111/j.1551-2916.2008.02469.x.

[13] H Hu, M Zhu, F Xie, N Lei, J Chen, Y Hou, H Yan. Effect of Co_2O_3 Additive on Structure and Electrical Properties of $85(Bi_{1/2}Na_{1/2})TiO_3$-$12(Bi_{1/2}K_{1/2})TiO_3$-$3BaTiO_3$ Lead-Free Piezoceramics. Journal of the American Ceramic Society. 2009;92:2039-2045. DOI: 10.1111/j.1551-2916.2009.03183.x.

[14] HY Tian, KW Kwok, HLW Chan, C E Buckley. The effects of CuO-doping on dielectric and piezoelectric properties of $Bi_{0.5}Na_{0.5}TiO_3$–$Ba(Zr,Ti)O_3$ lead-free ceramics. Journal of Materials Science. 2007;42:9750-9755. DOI: 10.1007/s10853-007-2005-z.

[15] DQ Xiao, DM Lin, JG Zhu, P Yu. Investigation on the design and

synthesis of new systems of BNT-based lead-free piezoelectric ceramics, Journal of Electronceramics. 2006; 16: 271-275. DOI: 10.1007/s10832-006-9863-7.

[16] D Lin, K W. Kwok. Ferroelectric and piezoelectric properties of $[(Bi_{0.98}La_{0.02}Na_{1-x}Li_x)_{0.5}]_{0.94}Ba_{0.06}TiO_3$ lead-free ceramics. Journal of Materials Science. 2009;44:4953-4958.

[17] SH Choy, XX Wang, HLW Chan, CL Choy. Electromechanical and ferroelectric properties of $(Bi_{1/2}Na_{1/2})TiO_3$-$(Bi_{1/2}K_{1/2})TiO_3$-$(Bi_{1/2}Li_{1/2})TiO_3$-$BaTiO_3$ lead-free piezoelectric ceramics for accelerometer application. Applied Physics A. 2007; 89: 775-781. DOI: 10.1007/s00339-007-4170-y.

[18] D Lin, Q Zheng, C Xu, K W. Kwok. Structure, electrical properties and temperature characteristics of $Bi_{0.5}Na_{0.5}TiO_3$–$Bi_{0.5}K_{0.5}TiO_3$–$Bi0.5Li_{0.5}TiO_3$ lead-free piezoelectric ceramics. Applied Physics A, 2008; 93: 549-558. DOI: 10.1007/s00339-008-4667-z.

[19] SB Vakhrushev, BG Ivanitskij, BE Kvyatkovskij, AN Majstrenko, RS Malysheva, NM Okuneva, NM Parfenova: Neutron scattering studies of the structure of sodium bismuth titanate. Soviet Physics Solid State, 1983; 25: 1504. (doi is not available)

[20] J. A. Zvirgzds, P. P. Kapostin, J. V. Zvirgzde, T. V. Kruzina. X-ray study of phase transitions in efrroelectric $Na_{0.5}Bi_{0.5}TiO_3$. Ferroelectrics, 1982; 40(1): 75-77. DOI: 10.1080/00150198208210600.

[21] Ljubomira Ana Schmitt, Hans-Joachim Kleebe: Single grains hosting two space groups—a transmission electron microscopy study of a lead-free ferroelectric. Functional Materials Letters. 2010;3:55-58. DOI: 10.1142/S1793604710000920.

[22] V. Dorcet, G. Trolliard, P. Boullay : Reinvestigation of phase transitions in $Na0.5Bi_{0.5}TiO_3$ by TEM. Part I: First order rhombohedral to orthorhombic phase transition. Chemistry of Materials. 2008;20:5061-5073. DOI: 10.1021/cm8004634.

[23] Koichiro Sakata, Yoichiro Masuda : Ferroelectric and antiferroelectric properties of $(Na_{0.5}Bi_{0.5})TiO_3$-$SrTiO_3$ solid solution ceramics. Ferroelectrics, 1974; 7(1): 347-349. DOI: 10.1080/00150197408238042

[24] ST Zhang, Alain Brice Kounga, Emil Aulbach : Giant strain in lead-free piezoceramics $Bi_{0.5}Na_{0.5}TiO_3$–$BaTiO_3$–$K_{0.5}Na_{0.5}NbO_3$ system. Applied Physics Letters. 2007;91:112906. DOI: 10.1063/1.2783200.

[25] F Gao, X Dong, C Mao, W Liu, H Zhang, L Yang, F Cao, and G Wang. Energy-storage properties of $0.89Bi_{0.5}Na_{0.5}TiO_3$-$0.06BaTiO_3$-$0.05K_{0.5}Na_{0.5}NbO_3$ lead-free anti-ferroelectric ceramics. Journal of the American Ceramic Society, 2011;94: 4382-4386. DOI: 10.1111/j.1551-2916.2011.04731.x.

[26] WJ Ren, Phase transition behaviors and energy-storage properties of BNT-BA-KNN ceramics, [thesis]. University of Chinese Academy of Sciences, 2016.

[27] YC Wu, YZ Fan, NT Liu, P Peng, MX Zhou, SG Yan, F Cao, XL Dong, GS Wang. Enhanced energy storage properties in sodium bismuth titanate-based ceramics for dielectric capacitor applications. Journal of Materials Chemistry C. 2019;7:6222-6230. DOI: 10.1039/C9TC01239G.

[28] S I Shkuratov, J Baird, V G Antipov, E F Talantsev, H R Jo, J C Valadez, C S Lynch. Depolarization mechanisms of $PbZr_{0.52}Ti_{0.48}O_3$ and $PbZr_{0.95}Ti_{0.05}O_3$ poled ferroelectrics under high strain rate loading. Applied Physics Letters. 2014;104: 212901. DOI: 10.1063/1.4879545.

[29] R E Setchell. Shock wave compression of the ferroelectric ceramic $Pb_{0.99}(Zr_{0.95}Ti_{0.05})_{0.98}Nb_{0.02}O_3$: depoling currents. Journal of Applied Physics, 2005;97:013507. DOI: 10.1063/1.1828215.

[30] SI Shkuratov, J Baird, V G Antipov, E F Talantsev, J B Chase, W Hackenberger, J Luo, H R Jo, C S Lynch. Ultrahigh energy density harvested from domain-engineered relaxor ferroelectric single crystals under high strain rate loading. Scientific Reports. 2017;7:46758. DOI: 10.1038/srep46758.

[31] ZP Gao, W Peng, B Chen, Simon A.T.Redfern, K Wang, BJ Chu, Q He, Y Sun, XF Chen, HC Nie, W Deng, LK Zhang, HL He, GS Wang, XL Dong. Giant power output in lead-free ferroelectrics by shock-induced phase transition. Physical Review Materials. 2019;3:2475-9953. DOI:10.1103/physrevmaterials.3.035401.

[32] Z Liu, W Ren, H Nie, P Peng, Y Liu, X Dong, F Cao, G Wang, Pressure driven depolarization behavior of $Bi_{0.5}Na_{0.5}TiO_3$ based lead-free ceramics. Applied Physics Letters, 2017;110: 212901. DOI:10.1063/1.4984088.

[33] P Peng, H Nie, W Guo, F Cao, G Wang, X Dong. Pressure-induced ferroelectric-relaxor phase transition in $(Bi_{0.5}Na_{0.5})TiO_3$-based ceramics. Journal of the American Ceramic Society. 2018.102:2569-2577. DOI:10.1111/jace.16069.

[34] P Peng, H Nie, G Wang, Z Liu, F Cao, X Dong. Shock-driven depolarization behavior in BNT-based lead-free ceramics. Applied Physics Letters. 2018. 113, 082901. DOI:10.1063/1.5045392.

[35] F Zhuo, Q Li, J Gao, Y Wang, Q Yan, Z Xia, Y Zhang, X Chu. Structural phase transition, depolarization and enhanced pyroelectric properties of $(Pb_{1-1.5x}La_x)(Zr_{0.66}Sn_{0.23}Ti_{0.11})O_3$ solid solution. Journal of Materials Chemistry C. 2016; 29:7110-7118. DOI: 10.1039/c6tc01326k.

[36] YX Tang, XY Zhao, XQ Feng, WQ Jin, HS Luo. Pyroelectric properties of 111-oriented $Pb(Mg_{1/3}Nb_{2/3})O_3$-$PbTiO_3$ crystals. Applied Physics Letters. 2005; 86:082901. DOI: 10.1063/1.1865337.

[37] YX Tang, LH Luo, YM Jia, HS Luo, XY Zhao, HQ Xu, D Lin, JL Sun, XJ Meng, JH Zhu, M Es-Souni. Mn-doped $_{0.71}Pb(Mg_{1/3}Nb_{2/3})O_3$-$0.29PbTiO_3$ pyroelectric crystals for uncooled infrared focal plane arrays applications. Applied Physics Letters. 2006;89: 162906. DOI: 10.1063/1.2363149.

[38] S Zhang, F Li. High performance ferroelectric relaxor-$PbTiO_3$ single crystals: Status and perspective. Journal of Applied Physics. 2012;111:031341. DOI: 10.1063/1.3679521.

[39] Y Li, Y Tang, J Chen, X Zhao, L Yang, F Wang, Z Zeng, H Luo. Enhanced pyroelectric properties and thermal stability of Mn-doped $0.29Pb(In_{1/2}Nb_{1/2})O_3$-$0.29Pb(Mg_{1/3}Nb_{2/3})O_3$-$0.42PbTiO_3$ single crystals. Applied Physics Letters. 2018; 112: 172901. DOI: 10.1063/1.5024286.

[40] M Kobune, A Mineshige, S Fujii, Y Maeda. Preparation and pyroelectric properties of Mn-modified (Pb, La)(Zr, Ti)O_3 (PLZT) ceramics. Japanese Journal of Applied Physics Part 1-Regular Papers Short Notes & Review Papers. 1997:36:5976-5980. DOI: 10.1143/JJAP.36.5976.

[41] H Chen, S Guo, X Dong, F Cao, C Mao, G Wang, $CaxSr_{0.3}$-$xBa_{0.7}Nb_2O_6$ lead-free pyroelectric ceramics with high depoling temperature. Journal of Alloys and Compounds. 2017; 695: 2723-2729. DOI: 10.1016/j.jallcom.2016.11.192.

[42] KS Srikanth, S Patel, S Steiner, Vaish R. Pyroelectric signals in (Ba,Ca)TiO_3-$xBa(Sn,Ti)O_3$ ceramics: A viable alternative for lead-based ceramics.

Scripta Materialia. 2018;146:146-149. DOI: 10.1016/j.scriptamat.2017.11.027.

[43] Y Tang, Z Shen, S Zhang, T R. Shrout, Improved Pyroelectric Properties of CaBi4Ti4O15 Ferroelectrics Ceramics by Nb/Mn Co-Doping for Pyrosensors. Journal of the American Ceramic Society. 2016;99:1294-1298. DOI: 10.1111/jace.14075.

[44] F Guo, B Yang, S Zhang, F Wu, D Liu, P Hu, Y Sun, D Wang, W Cao. Enhanced pyroelectric property in (1-x) ($Bi_{0.5}Na_{0.5}$) $TiO_{3-x}Ba(Zr_{0.055}Ti_{0.945})O_3$: Role of morphotropic phase boundary and ferroelectric-antiferroelectric phase transition. Applied Physics Letters. 2013; 103: 182906. DOI: 10.1063/1.4828675.

[45] AM Balakt, CP Shaw and Q Zhang. Giant pyroelectric properties in La and Ta co-doped lead-free $0.94Na_{0.5}Bi_{0.5}TiO_3$-$0.06BaTiO_3$ ceramics. Journal of Alloys and Compounds. 2017;709: 82-91. DOI: 10.1016/j.jallcom.2017.03.143

[46] AM Balakt, CP Shaw and Q Zhang. The decrease of depolarization temperature and the improvement of pyroelectric properties by doping Ta in lead-free $0.94Na_{0.5}Bi_{0.5}TiO_3$-$0.06BaTiO_3$ ceramics. Ceramics International. 2017;43: 3726-33. DOI: 10.1016/j.ceramint.2016.12.004.

[47] AM Balakt, CP Shaw and Q Zhang. Enhancement of pyroelectric properties of lead-free 0.94 Na0.5Bi0.5TiO3-0.06 $BaTiO_3$ ceramics by La doping. Journal of the European Ceramic Society. 2017;37:1459-66. DOI: 10.1016/j.jeurceramsoc.2016.12.021.

[48] M Kobune, A Mineshige, S Fujii and Y Maeda. Preparation and pyroelectric properties of Mn-modified (Pb, La) $(Zr, Ti)O_3$ (PLZT) ceramics. Japanese Journal of Applied Physics Part 1-Regular Papers Short Notes & Review Papers. 1997;36:5976-80. DOI: 10.1143/JJAP.36.5976.

[49] Y Li, Y Tang, J Chen, X Zhao, L Yang, F Wang, Z Zeng and H Luo. Enhanced pyroelectric properties and thermal stability of Mndoped $0.29Pb(In_{1/2}Nb_{1/2})O_3$-$0.29Pb(Mg_{1/3}Nb_{2/3})O_3$-$0.42PbTiO_3$ single crystals. Applied Physics Letters. 2018; 112:172901. DOI: 10.1063/1.5024286.

[50] J Jia, S Guo, F Cao, S Yan, C Yao, X Dong, G Wang. The improved pyroelectric properties, high depolarization temperature and excellent thermal stability in lead-free $(1-x)(Bi_{0.5}Na_{0.5})TiO_3$-$xBa(Ni_{0.5}Nb_{0.5})O_3$ ceramics. Materials Research Express. 2019;6:046308. DOI: 10.1088/2053-1591/aafcd0.

[51] J Jia, S Guo, S Yan, F Cao, C Yao, X Dong, G Wang. Simultaneous large pyroelectric response and high depolarization temperature in sodium bismuth titanate-based perovskites. Applied Physics Letters. 2019;114:032902. DOI: 10.1063/1.5063318.

[52] P Peng, H Nie, Z Liu, F Cao, G Wang, X Dong. Enhanced pyroelectric properties in $(Bi_{0.5}Na_{0.5})TiO_3$–$BiAlO_3$–$NaNbO_3$ ternary system lead-free ceramics. Journal of the American Ceramic Society. 2018;101:4044-4052. DOI: 10.1111/jace.15568.